

Supporting Information

Detection of phosphorylation states by intermolecular sensitization of lanthanide-peptide conjugates

Elena Pazos,^a Marko Goličnik,^b José L. Mascareñas*^a and M. Eugenio Vázquez*^a

^a *Centro Singular de Investigación en Química Biolóxica e Materiais Moleculares, Departamento de Química Orgánica and Unidad Asociada al CSIC. Universidade de Santiago de Compostela, 15782 Santiago de Compostela. Spain. Fax: +34 981 505 012; Tel: +34 881 815 738; E-mail: joseluis.mascarenas@usc.es, eugenio.vazquez@usc.es*

^b *Institute of Biochemistry, Faculty of Medicine, University of Ljubljana, Vrazov trg 2, 1000 Ljubljana, Slovenia. Fax: +386 1 5437641; Tel: +386 1 5437669; E-mail: marko.golicnik@mf.uni-lj.si*

General ligand and peptide synthesis procedures

All peptide synthesis reagents and amino acid derivatives were purchased from *GL Biochem* (Shanghai) and *NovaBiochem*; standard amino acids were purchased as protected Fmoc amino acids with the standard side chain protecting scheme: Fmoc-Trp(Boc)-OH, Fmoc-Pro-OH, Fmoc-Gly-OH, Fmoc-Ser(*t*Bu)-OH, Fmoc-Phe-OH and Fmoc-Arg(Pbf)-OH. The Fmoc-Ser(PO(OBzl)OH)-OH was purchased from *Bachem* (Cat. #: B-3455) and the orthogonally protected Fmoc-Asp(OAll)-OH and Fmoc-Glu(OAll)-OH were purchased from *Aldrich* (Cat. #: 47579 and 47703 respectively). C-terminal amide peptides were synthesized on a 0.05 mmol scale using a 0.21 mmol/g loading Fmoc-PAL-PEG-PS resin from *Applied Biosystems*. All other chemicals were purchased from *Aldrich* or *Fluka*. All solvents were dry and synthesis grade, except DMF for peptide synthesis.

Peptides were synthesized using a *PS3* automatic peptide synthesizer from *Protein Technologies*. The amino acids were coupled in 4-fold excess using 2-[(1*H*-benzotriazol-1-yl)-1,1,3,3-tetramethyluronium hexafluorophosphate (HBTU) as activating agent. DO3A(*t*Bu)₃-propylamino derivative (**3**) was coupled manually in 4-fold excess using 2-(1*H*-7-aza-benzotriazol-1-yl)-1,1,3,3-tetramethyluronium hexafluorophosphate (HATU) as activating agent. Each amino acid was activated for 30 seconds in DMF before being added onto the resin. Peptide bond-forming couplings were conducted for 30 min to 45min. The deprotection of the temporal Fmoc protecting group was performed by treating the resin with 20% piperidine in DMF solution for 10 min. The final peptides were cleaved from the resin, and side-chain protecting groups were simultaneously removed using a standard TFA cleavage cocktail as outlined below.

High-Performance Liquid Chromatography (HPLC) was performed using an *Agilent 1100* series Liquid Chromatograph Mass Spectrometer system. Analytical HPLC was run using a *Zorbax Eclipse XDB-C₈* (5 μm) 4.6 × 150 mm analytical column from *Agilent*. The purification of the peptides was performed on a *Jupiter Proteo 90A* (4 μm) 10 × 250 mm reverse-phase column from *Phenomenex*. The standard gradient used for analytical and preparative HPLC was 15→95% CH₃CN, 0.1% TFA / H₂O, 0.1% TFA over 30 min. Electrospray Ionization Mass Spectrometry (ESI/MS) was performed with an *Agilent 1100 Series LC/MSD VL G1956A* model in positive scan mode using direct injection of the purified peptide solution.

The chelating macrocycle **3** was purified in a *Büchi Sepacore* preparative system consisting on a pump manager *C-615* with two pump modules *C-605* for binary solvent gradients, a fraction collector *C-660*, and UV Photometer *C-635*. Purification was made using a reverse phase linear

gradient of 25 → 95% MeOH, 0.1% TFA / H₂O, 0.1% TFA over 30 min, using a pre-packed preparative cartridge (75 × 40 mm) with reverse phase RP-18 silica gel (*Büchi* order #: 54862).

UV measurements were made in a Varian *Cary 100 Bio* spectrophotometer, using a standard *Hellma* semi-micro cuvette. Concentrations were measured using the listed extinction coefficient for Trp: 5579 M⁻¹cm⁻¹ at 278 nm.¹

The luminescence experiments were made with different experimental setups:

Setup 1: Steady-state emission measurements were made with a *Jobin-Yvon Fluoromax-3*, (DataMax 2.20), coupled to a *Wavelength Electronics* LFI-3751 temperature controller. All measurements were made with a *Hellma* semi-micro cuvette (114F-QS) at 20 °C, using the following settings: excitation wavelength 280 nm; excitation slit width 4.0 nm, emission slit width 5.0 nm; increment 1.0 nm; integration time 0.20 s. The emission spectra were recorded from 450 to 600 nm with a 370 nm long-pass filter to avoid interference from harmonic doubling.

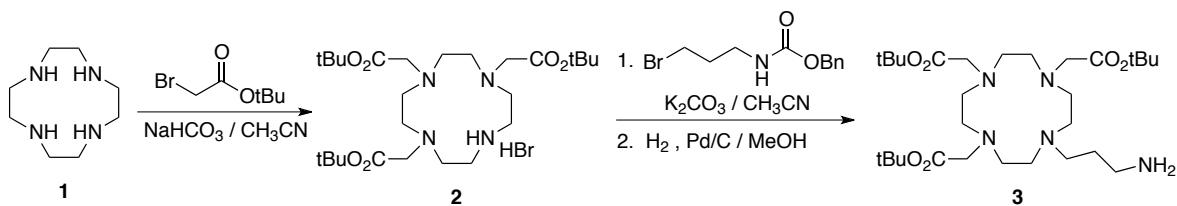
Setup 2: Time-gated emission measurements were made with a *Varian Cary Eclipse* Fluorescence Spectrophotometer. All measurements were made with a *Hellma* semi-micro cuvette (114F-QS) at rt, using the following settings: excitation wavelength 280 nm; increment 1.0 nm; average time 0.1 s; total decay time 0.02 s; delay time 0.2 ms; gate time 5 ms; PMT detector voltage 800 v. The emission spectra for terbium and europium complexes were recorded from 450 to 600 nm and 550 to 750 nm respectively.

Setup 3: Lifetime experiments were made with a *Varian Cary Eclipse* Fluorescence Spectrophotometer. All measurements were made with a *Hellma* semi-micro cuvette (114F-QS) at rt, using the following settings: excitation wavelength 280 nm; emission wavelength 545 nm; excitation slit width 20.0 nm, emission slit width 10.0 nm; total decay time 15.0 ms; delay time 0.05 ms; gate time 0.2 ms; number of cycles 500; PMT detector voltage 800 v.

Setup 4: Kinetic experiments were made with a *Varian Cary Eclipse* Fluorescence Spectrophotometer. All measurements were made with a *Hellma* semi-micro cuvette (114F-QS) at rt, using the following settings: excitation wavelength 280 nm; emission wavelength 616 nm; excitation slit width 2.5 nm, emission slit width 1.5 nm; average time 1.0 s; total decay time 0.02 s; delay time 0.2 ms; gate time 5 ms; PMT detector voltage 800 V.

¹ G. D. Fasman, *Handbook of Biochemistry and Molecular Biology, Proteins*, I 1976, CRC Press, 3 ed., pp. 183–203.

Synthesis of the DO3A(*t*Bu)₃-propylamino ligand (**3**)



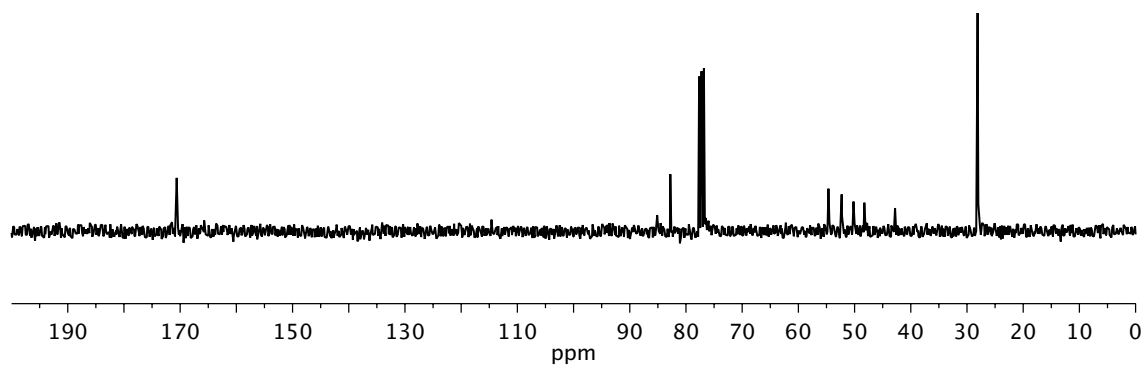
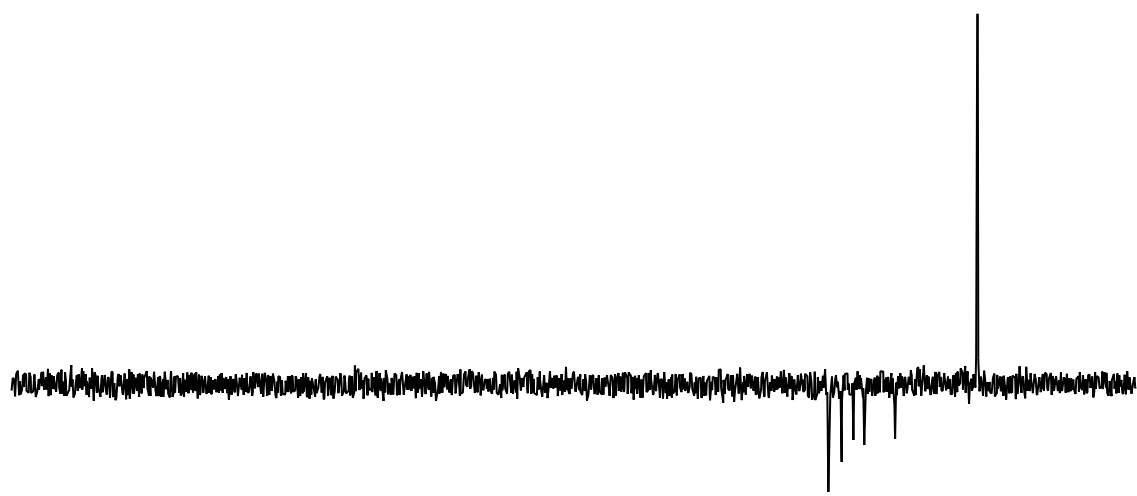
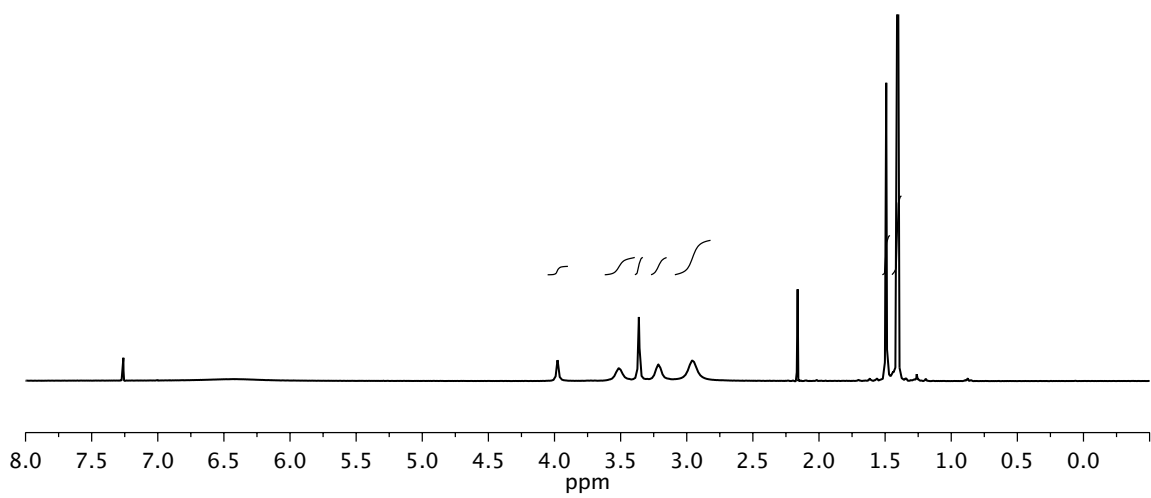
1,4,7-Tris(*tert*-butoxycarbonylmethyl)-1,4,7,10-tetraazacyclododecane (**2**) was prepared according to procedures described in literature.² Thus, 1,4,7,10-tetraazacyclododecane (**1**, 1.78 g, 10 mmol) and sodium hydrogen carbonate (2.78 g, 33 mmol) were stirred in freshly distilled acetonitrile (60 mL) under argon, the mixture was cooled to 0 °C. *Tert*-butyl bromoacetate (6.45 g, 33 mmol) was added dropwise over 45 min. The reaction mixture was stirred under argon for 48 h. The inorganic solids were removed by filtration and the filtrate evaporated under reduced pressure. Recrystallization from toluene afforded the desired product as a white solid (1.96 g, 33%).

¹H RMN (300 MHz, CDCl₃) δ: 1.41 (s, 18H), 1.49 (s, 9H), 2.96 (broad s, 8H), 3.22 (broad s, 4H), 3.36 (s, 4H), 3.51 (broad s, 4H), 3.98 (s, 2H).

¹³C RMN (75.5 MHz, CDCl₃) δ: 28.1 (CH₃), 42.8 (CH₂), 48.3 (CH₂), 50.2 (CH₂), 52.3 (CH₂), 54.7 (CH₂), 82.8 (C), 170.6 (CO).

HRMS-ESI (m/z): [MH]⁺ calcd for C₂₆H₅₁N₄O₆ 515.3730, found 515.3773.

² A. Dadabhoy, S. Faulkner and P. Sammes, *J. Chem. Soc., Perkin Trans. 2*, 2002, 348.



1,4,7-Tris(*tert*-butoxycarbonylmethyl)-10-(3-aminopropyl)-1,4,7,10-tetraazacyclododecane (**3**) was synthesized according to the literature.³ 1,4,7-tris(*tert*-butoxycarbonylmethyl)-1,4,7,10-tetraazacyclododecane (**2**, 150 mg, 0.25 mmol) was dissolved in freshly distilled acetonitrile (10 mL). Potassium carbonate (104 mg, 0.75 mmol) and benzyl 3-bromopropylcarbamate (137 mg, 0.50 mmol) were added and the mixture was refluxed under Ar for 16 h. The inorganic solids were removed by filtration and the filtrate evaporated under reduced pressure to give a pale-yellow oil, which was purified by flash column chromatography in silica (4% MeOH/CH₂Cl₂).⁴ The isolated product was dissolved in MeOH (10 mL), Pd/C (27 mg, 10%) was added to the solution, and the mixture was stirred at room temperature under a hydrogen atmosphere for 16 h (balloon pressure). The reaction mixture was filtered through celite, concentrated under reduced pressure and purified in a preparative system in reverse phase (25 → 95% MeOH, 0.1% TFA / H₂O, 0.1% TFA over 30 min) to give a pale yellow solid (64 mg, 44%).

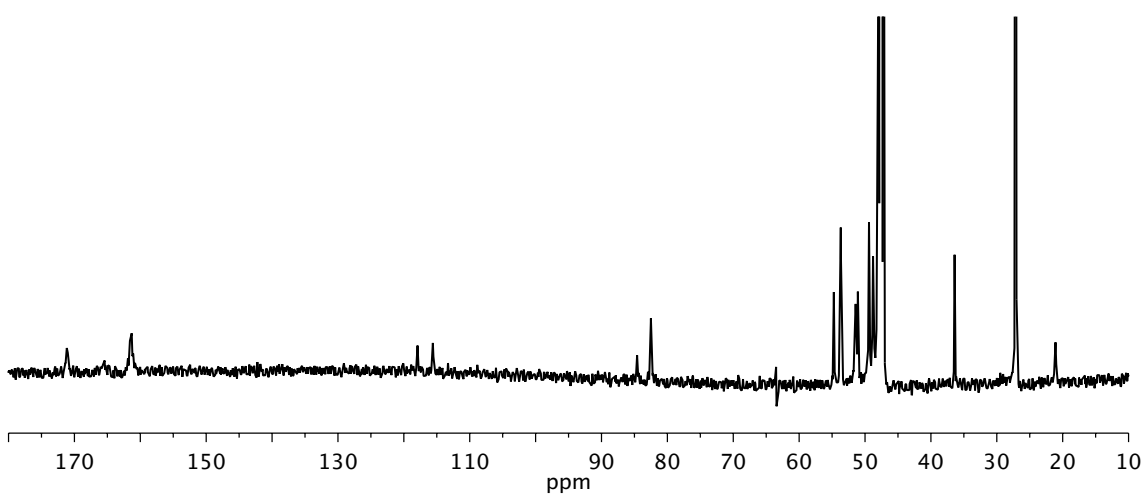
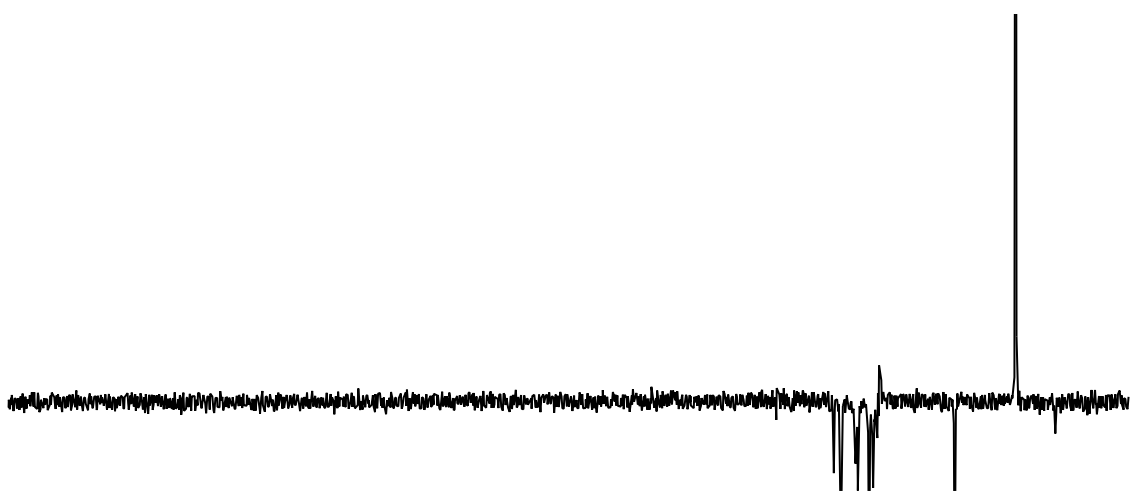
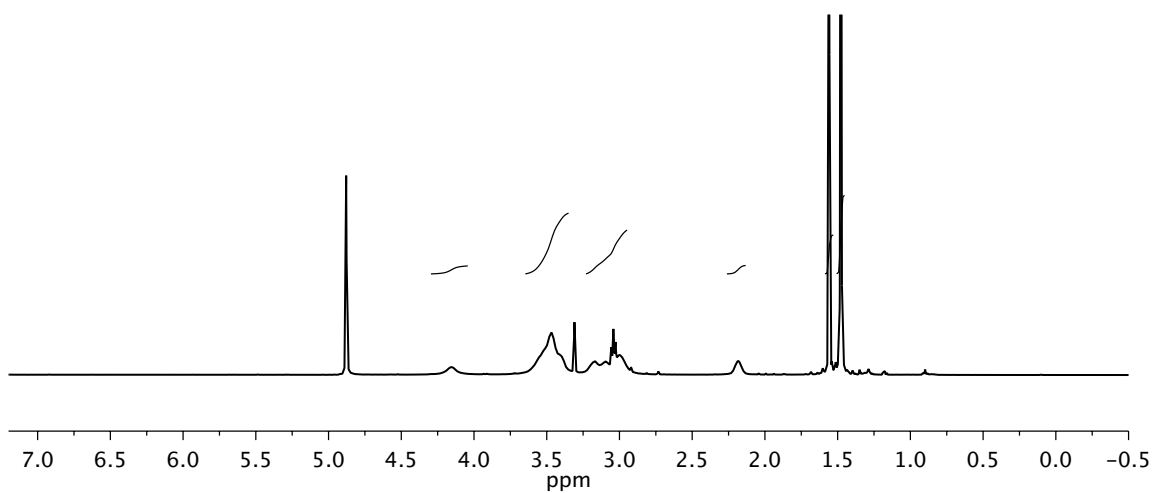
¹H RMN (500 MHz, CD₃OD) δ: 1.48 (s, 18H), 1.56 (s, 9H), 2.18 (broad s, 2H), 2.95-3.23 (m, 10H), 3.35-3.65 (m, 14H), 4.16 (broad s, 2H).

¹³C RMN (125.8 MHz, CD₃OD) δ: 21.1 (CH₂), 27.1 (CH₃), 36.4 (CH₂), 48.8 (CH₂), 49.4 (CH₂), 51.1 (CH₂), 51.4 (CH₂), 53.7 (CH₂), 54.7 (CH₂), 82.5 (C), 84.6 (C), 161.3 (CO), 171.2 (CO).

HRMS-ESI (m/z): [MH]⁺ calcd for C₂₉H₅₈N₅O₆ 572.4309, found 572.4355.

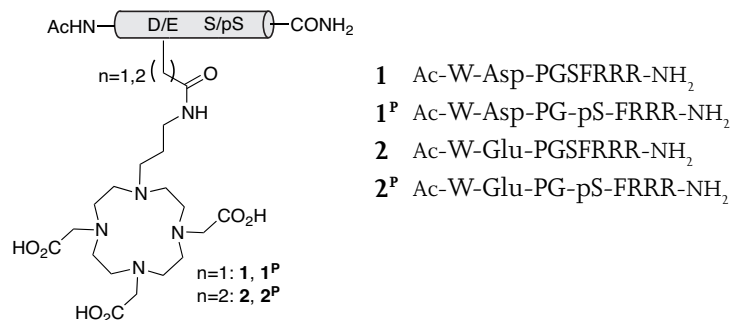
³ K. Dhingra, P. Fouskova, G. Angelovski, M. E. Maier, N. K. Logothetis and E. Tóth, *J. Biol. Inorg. Chem.*, 2007, **13**, 35.

⁴ W. C. Still, M. Kahn and A. Mitra, *J. Org. Chem.*, 1978, **23**, 2923.

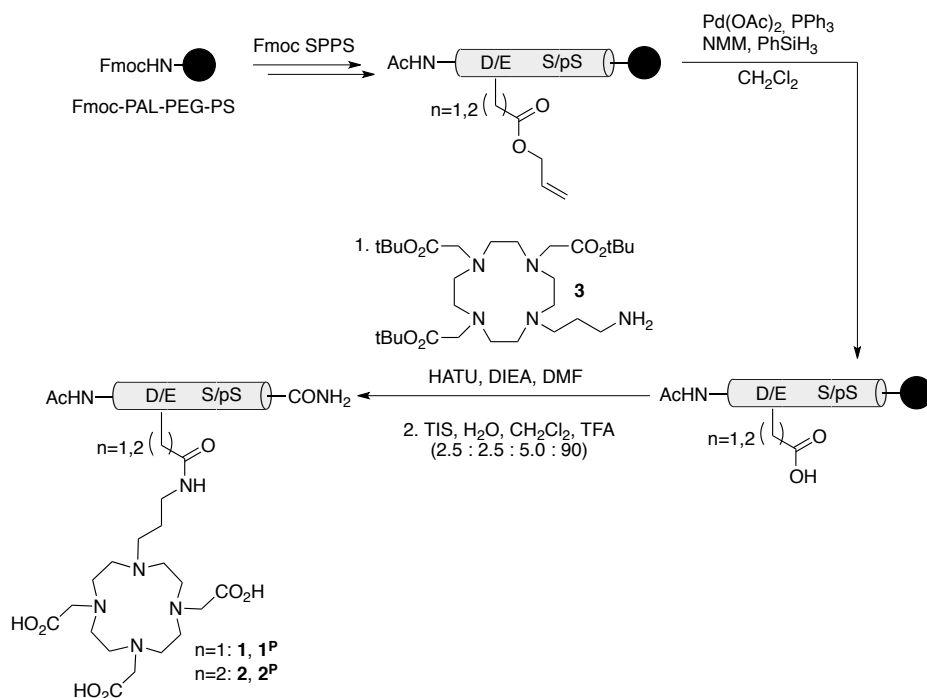


Outline of the peptide synthesis strategies

The sequences of the different peptides are:



The strategy for the synthesis of side-chain DO3A-propylamino-conjugated peptides **1**, **1^P**, **2** and **2^P** involved a modified protecting group scheme of the standard Fmoc solid phase peptide synthesis procedures. The aspartic and glutamic acid residues were introduced as their sidechain allyl-protected derivatives, which allowed its selective deprotection (Pd catalysis) and derivatization in the solid phase with the DO3A(*t*Bu)₃-propylamino macrocycle (**3**).



Scheme S1: Synthesis of the peptides **1**, **1^P**, **2** and **2^P** with the DO3A unit orthogonally attached to the Asp side chain (**1** and **1^P**) or to the Glu side chain (**2** and **2^P**).

Acetylation of the N-terminus: After the final Fmoc deprotection step using standard conditions (20% piperidine/DMF), the peptides (0.05 mmol) were acetylated by treatment with 20% Ac₂O in DMF (2.5 mL) and 0.195 M *N,N*-diisopropylethylamine (DIEA) in DMF (1.75 mL) for 45 min. After filtration, the resin was washed with DMF (3 × 5 mL × 3 min) and CH₂Cl₂ (3 × 5 mL × 3 min) and dried under a current of argon.

Deprotection of the orthogonally protected Asp(OAll) and Glu(OAll) side chains: Once the peptides were fully assembled in the solid phase, the side chains of the Asp(OAll) and Glu(OAll) residues were selectively deprotected for specific attachment of the ligand to each peptide, following in all cases the same procedure: 0.05 mmol of peptide attached to the solid support were treated at room temperature for 11 h with a mixture of Pd(OAc)₂ (0.3 eq), PPh₃ (1.5 eq), *N*-methylmorpholine (10 eq) and PhSiH₃ (10eq) in CH₂Cl₂ (2.5 mL). The resin was then filtered and washed with THF (1 × 5 mL × 2 min), DMF (2 × 5 mL × 2 min), diethyldithiocarbamate (DEDTC) (25 mg in 5 mL of DMF, 2 × 5 min), DMF (2 × 5 mL × 2 min), and CH₂Cl₂ (2 × 5 mL × 2 min).

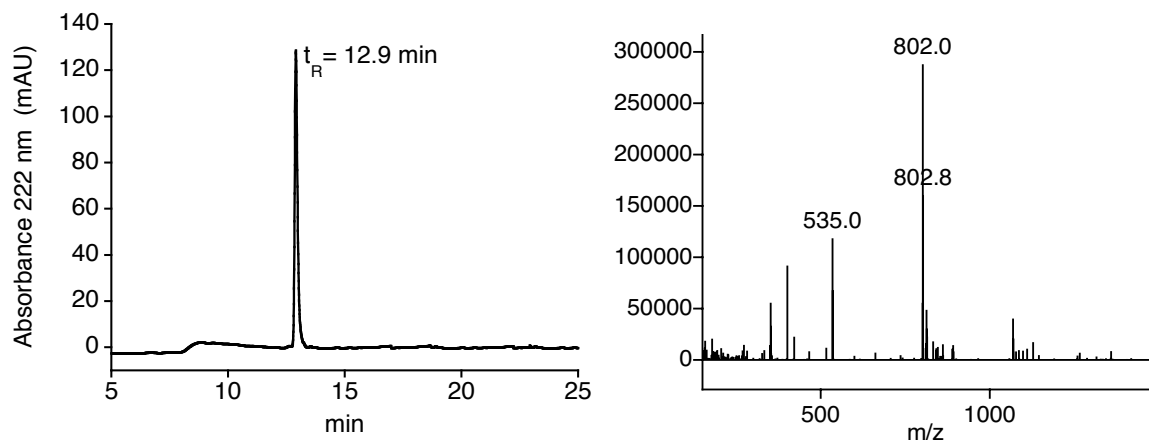
DO3A(*t*Bu)₃-propylamino ligand coupling: The allyl-deprotected peptides attached to the resins (0.01 mmol) were suspended in dry DMF (0.5 mL). HATU (3.8 mg, 0.01 mmol) and 0.195 M DIEA in DMF (77 μL, 0.015 mmol) were added to the solution. After five minutes, DO3A(*t*Bu)₃-propylamino derivative (**3**, 17 mg, 0.03 mmol) was added to the mixture and the resin suspension was shaken for 4 h. After filtration, the resin was washed with DMF (3 × 1 mL × 3 min) and CH₂Cl₂ (3 × 1 mL × 3 min), and dried under argon.

Cleavage and deprotection of semipermanent protecting groups: The resin-bound peptide, dried overnight (0.01 mmol), was placed in a 50 mL falcon tube to which 1.5 mL of the cleavage cocktail (75 μL of CH₂Cl₂, 37.5 μL of water, 37.5 μL of triisopropylsilane (TIS) and TFA to 1.5 mL) were added. The resulting mixture was shaken for 3.5 h. The resin was then filtered, and the TFA filtrate was concentrated under argon current to a volume of approximately 1 mL. The residue was added to ice-cold diethyl ether (20 mL). After 10 min the precipitate was centrifuged and washed again with 10 mL of ice-cold ether and centrifuged. The solid residue was dried under argon and redissolved in acetonitrile/water 1:1 (1 mL) and purified by preparative reverse-phase HPLC. The collected fractions were lyophilized and stored at -20 °C.

HPLC purification of each crude gave a white solid, which was identified as the desired product by MS.

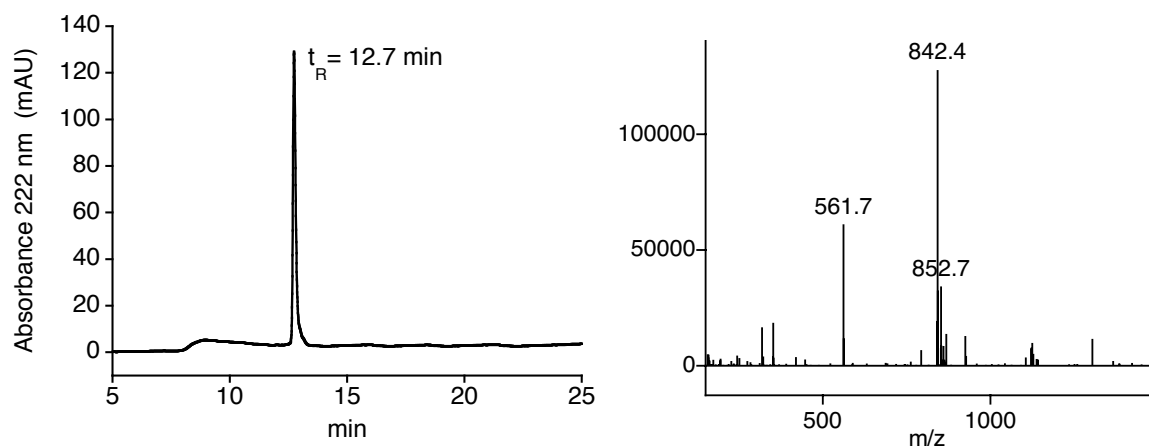
1: ESI-MS (m/z): $[\text{MH}]^+$ calcd for $\text{C}_{71}\text{H}_{112}\text{N}_{25}\text{O}_{18}$ = 1602.9, found = 802.0 $[\text{MH}_2]^{2+}$; 535.0 $[\text{MH}_3]^{3+}$.

UV (H_2O) λ_{max} , nm (ϵ): 278 (5579) $\text{M}^{-1}\text{cm}^{-1}$ (2.9 mg, 18% yield for 0.01 mmol scale).

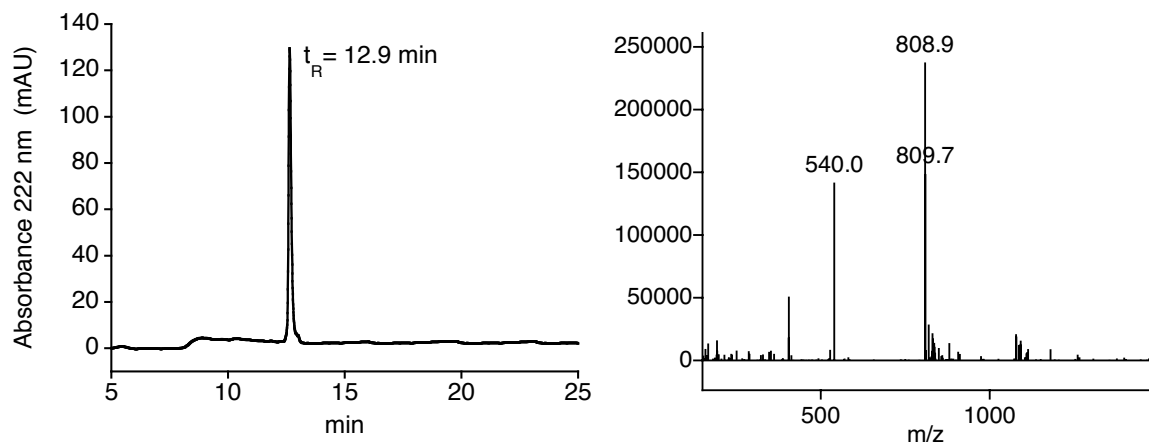


1^P: ESI-MS (m/z): $[\text{MH}]^+$ calcd for $\text{C}_{71}\text{H}_{113}\text{N}_{25}\text{O}_{21}\text{P}$ = 1682.8, found = 842.4 $[\text{MH}_2]^{2+}$; 561.7

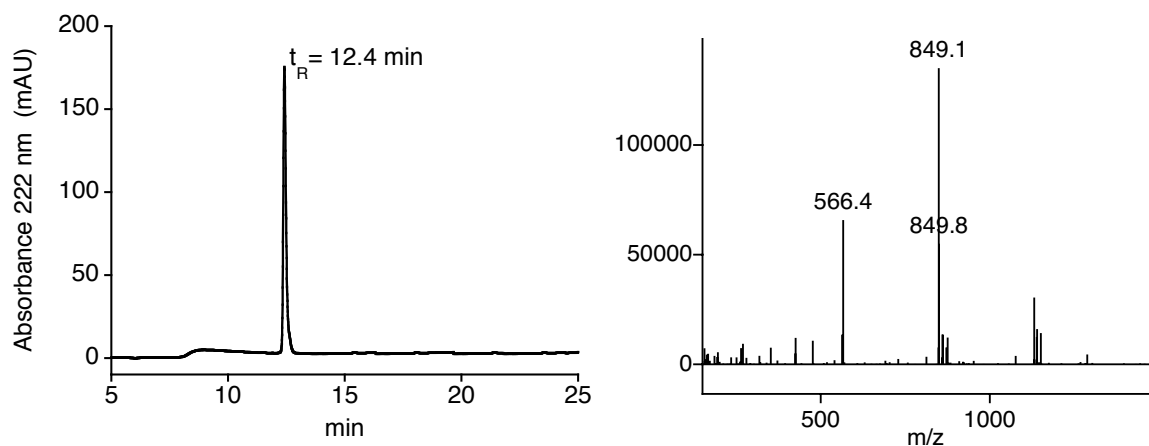
$[\text{MH}_3]^{3+}$. UV (H_2O) λ_{max} , nm (ϵ): 278 (5579) $\text{M}^{-1}\text{cm}^{-1}$ (3.5 mg, 21% yield for 0.01 mmol scale).



2: ESI-MS (m/z): $[\text{MH}]^+$ calcd for $\text{C}_{72}\text{H}_{114}\text{N}_{25}\text{O}_{18}$ = 1616.9, found = 808.9 $[\text{MH}_2]^{2+}$; 540.0 $[\text{MH}_3]^{3+}$.
UV (H_2O) λ_{max} , nm (ϵ): 278 (5579) $\text{M}^{-1}\text{cm}^{-1}$ (4.3 mg, 27% yield for 0.01 mmol scale).



2^P: ESI-MS (m/z): $[\text{MH}]^+$ calcd for $\text{C}_{72}\text{H}_{115}\text{N}_{25}\text{O}_{21}\text{P}$ = 1696.8, found = 849.1 $[\text{MH}_2]^{2+}$; 566.4 $[\text{MH}_3]^{3+}$. UV (H_2O) λ_{max} , nm (ϵ): 278 (5579) $\text{M}^{-1}\text{cm}^{-1}$ (4.1 mg, 24% yield for 0.01 mmol scale).



Luminescence assays

Luminescent experiments for detecting the formation of Tb complexes 1[Tb], 1^P[Tb], 2[Tb] and 2^P[Tb]: To 1 mL of a 10 μM solution of each peptide, **1**, **1^P**, **2** and **2^P**, in HEPES buffer (10 mM HEPES, 100 mM NaCl, pH 7.6), aliquots of a 1 mM stock solution of TbCl₃ were successively added at 20 °C, and the luminescence spectra were recorded after each addition using *setup 1* parameters.

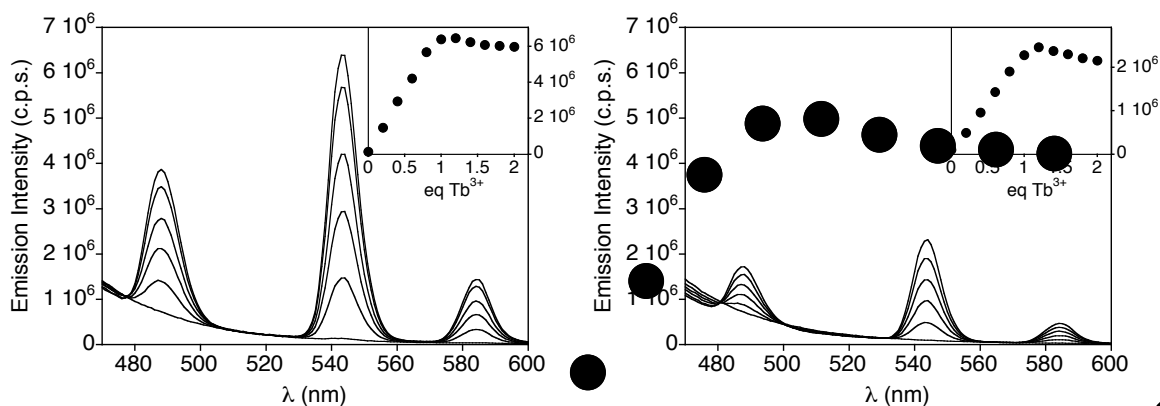


Figure S1. Luminescent spectra of **1** (left) and **1^P** (right), adding increasing amounts of TbCl₃, both peptides in 10 μM concentration in HEPES buffer (10 mM HEPES, 100 mM NaCl, pH 7.6), $\lambda_{\text{exc}} = 280$ nm. Inset is represented the emission at 545 nm with increasing amounts of TbCl₃, showing the complete formation of the terbium complexes with 1 eq of metal.

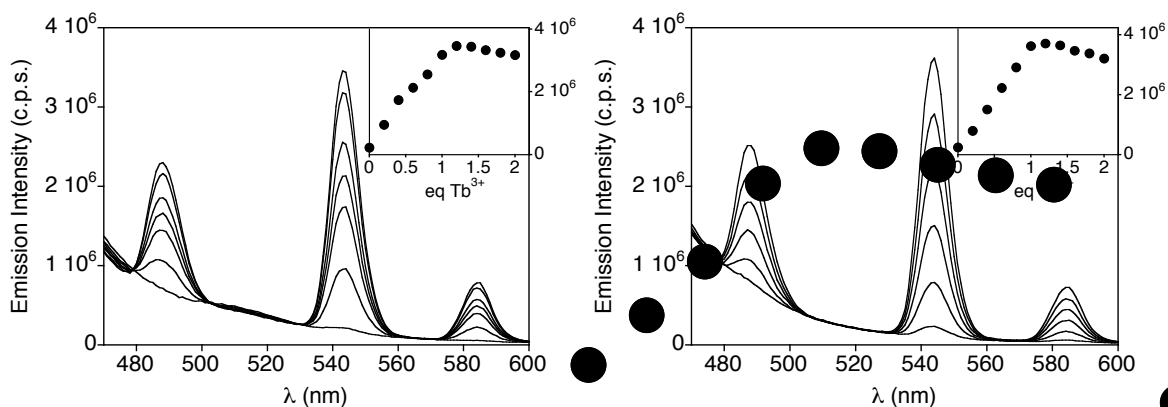


Figure S2. Luminescent spectra of **2** (left) and **2^P** (right), adding increasing amounts of TbCl₃, both peptides in 10 μM concentration in HEPES buffer (10 mM HEPES, 100 mM NaCl, pH 7.6), $\lambda_{\text{exc}} = 280$ nm. Inset is represented the emission at 545 nm with increasing amounts of TbCl₃, showing the complete formation of the terbium complexes with 1 eq of metal.

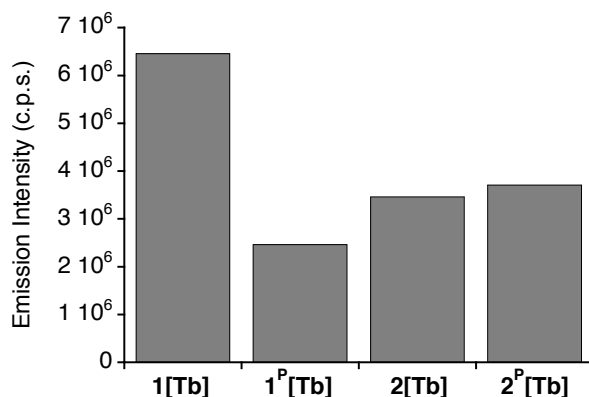


Figure S3. Bar graph of the luminescence emission at 545 nm of 10 μM solutions of each peptide, **1[Tb]**, **1^P[Tb]**, **2[Tb]** and **2^P[Tb]**, in HEPES buffer (10 mM HEPES, 100 mM NaCl, pH 7.6) upon irradiation at 280 nm.

Determination of the number of Tb^{3+} -coordinated water molecules for 1[Tb] and 1^P[Tb]: The decay data of the emission intensity at 545 nm were fit to a single exponential decay of the form: $I(t) = I(0)e^{(-t/\tau)}$, where $I(t)$ is the intensity at time t after the excitation pulse, $I(0)$ is the initial intensity at $t = 0$, and τ is the luminescence lifetime.

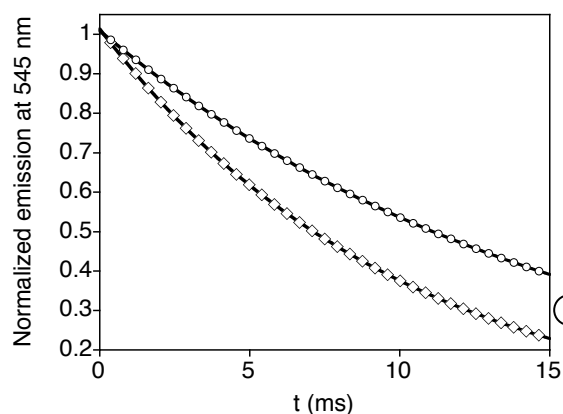


Figure S4. Emission decay of **1[Tb]** at 545 nm with time. (\diamond) Sample in 100% H_2O ; (\circ) sample in 80% D_2O .

The number of water molecules (q) can be estimated by measuring the rate constant of luminescence decay (τ^{-1}) in both H_2O and D_2O solutions, and fitting to the equation:⁵

⁵ R. J. Aarons, J. K. Notta, M. M. Meloni, J. Feng, R. Vidyasagar, J. Narvainen, S. Allan, N. Spencer, R. A. Kauppinen, J. S. Snaith and S. Faulkner, *Chem. Commun.*, 2006, 909; A. Beeby, I. M. Clarkson, R. S. Dickens, S. Faulkner, D. Parker, L. Royle, A. S. de Sousa, J. A. G. Williams and M. Woods, *J. Chem. Soc., Perkin Trans. 2*, 1999, 493.

$$q = A'(\Delta k_{\text{corr}}), \text{ where } A' = 5 \text{ ms and } \Delta k_{\text{corr}} = (k_{\text{H}_2\text{O}} - k_{\text{D}_2\text{O}} - 0.06 \text{ ms}^{-1}) \text{ for } \text{Tb}^{3+}.$$

The value for τ^{-1} in D_2O was estimated by measuring the lifetime of $\mathbf{1}[\text{Tb}]$ and $\mathbf{1}^{\text{P}}[\text{Tb}]$ in solutions of varying $\text{H}_2\text{O}:\text{D}_2\text{O}$ ratios from 0.2 to 1. The y-intercept of a plot of τ^{-1} vs the mole fraction of H_2O corresponds to the value in pure D_2O .

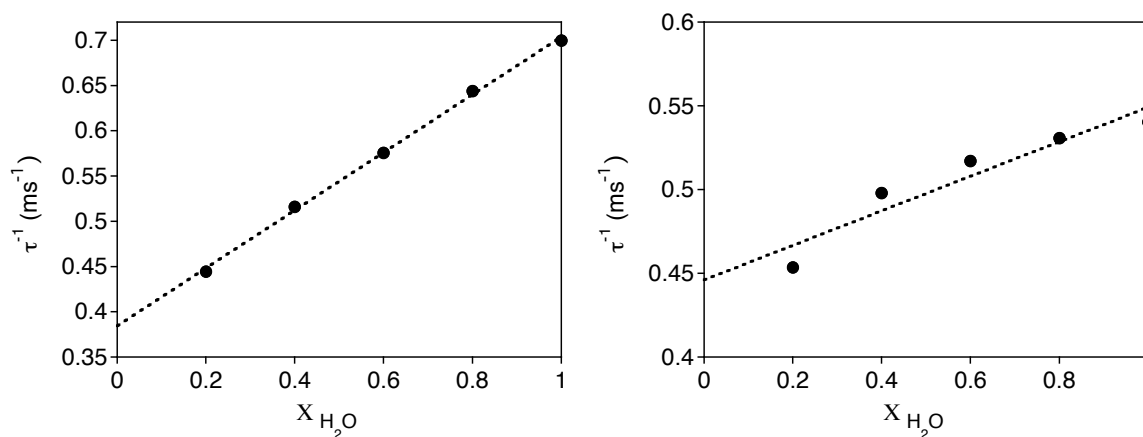


Figure S5. Representation of τ^{-1} against the mole fraction of H_2O for $\mathbf{1}[\text{Tb}]$ (left) and $\mathbf{1}^{\text{P}}[\text{Tb}]$ (right).

Compound	τ (H_2O)	τ (D_2O)	q
$\mathbf{1}[\text{Tb}]$	1.43 ms	2.60 ms	1.27
$\mathbf{1}^{\text{P}}[\text{Tb}]$	1.85 ms	2.24 ms	0.17

Table S1. Obtained values of the luminescence lifetime, in H_2O and D_2O , and number of Tb^{3+} -coordinated water molecules for $\mathbf{1}[\text{Tb}]$ and $\mathbf{1}^{\text{P}}[\text{Tb}]$.

Serial dilutions of $\mathbf{1}^{\text{P}}[\text{Tb}]$. Our working model is based on the intramolecular coordination of the phosphate anion to the terbium ion. In order to rule out the possibility of a dimeric $(\mathbf{1}^{\text{P}}[\text{Tb}])_2$ emissive complex in which the phosphate of one peptide is coordinating the $\text{DO3A}[\text{Tb}]$ complex of the second peptide, we measured the luminescence emission of a series of progressively more diluted solutions of the $\mathbf{1}^{\text{P}}[\text{Tb}]$ peptide HEPES buffer. If the dimeric $(\mathbf{1}^{\text{P}}[\text{Tb}])_2$ species were responsible for the luminescence, then it would not be linearly dependent on the concentration because it would affect the equilibrium between monomeric and dimeric states. As expected, the emission of $\mathbf{1}^{\text{P}}[\text{Tb}]$ solutions ranging from $10 \mu\text{M}$ to 5 nM displayed excellent linear dependency with the total peptide concentration indicating that the peptides do not dimerize (Figure S6). Likewise, introduction of a dimerization equilibrium in the titration profile of $\mathbf{1}^{\text{P}}$ with Tb did not

result in a good fit to the experimental data in the titration, further supporting the hypothesis of a monomeric $1^P[\text{Tb}]$ emissive complex.

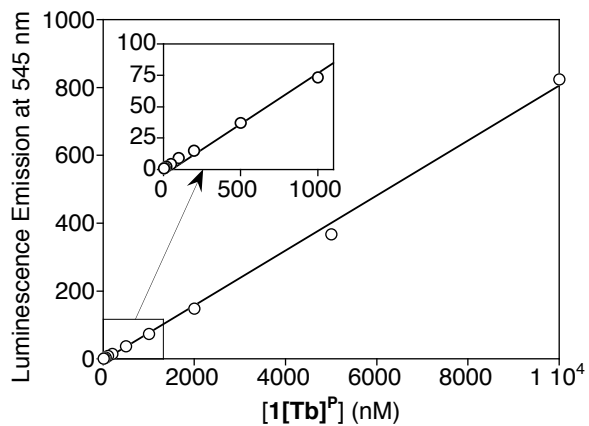


Figure S6. Luminescence emission a series of $1^P[\text{Tb}]$ solutions in HEPES buffer (10 mM HEPES, 100 mM NaCl, pH 7.6), and best fit to a linear equation ($\lambda_{\text{exc}} = 280 \text{ nm}$).

Luminescent experiments for detecting the formation of Eu complexes, $1[\text{Eu}]$ and $1^{\text{P}}[\text{Eu}]$, with an external antenna: To 1 mL of a 10 μM solutions of **1** and 1^{P} in HEPES buffer (10 mM HEPES, 100 mM NaCl, pH 7.6), 10 μL of a 1 mM stock solution of EuCl_3 were added and stirred for 1 hour. To each 10 μM solution of $1[\text{Eu}]$ and $1^{\text{P}}[\text{Eu}]$, aliquots of a 1 mM stock solution of 4,4,4-trifluoro-1-(2-naphthyl)-1,3-butanedione (**TNB**) in MeOH were successively added at rt, and the luminescence spectra were recorded after each addition using *setup 2* parameters with an excitation slit width of 2.5 nm and an emission slit width of 2.5 nm.

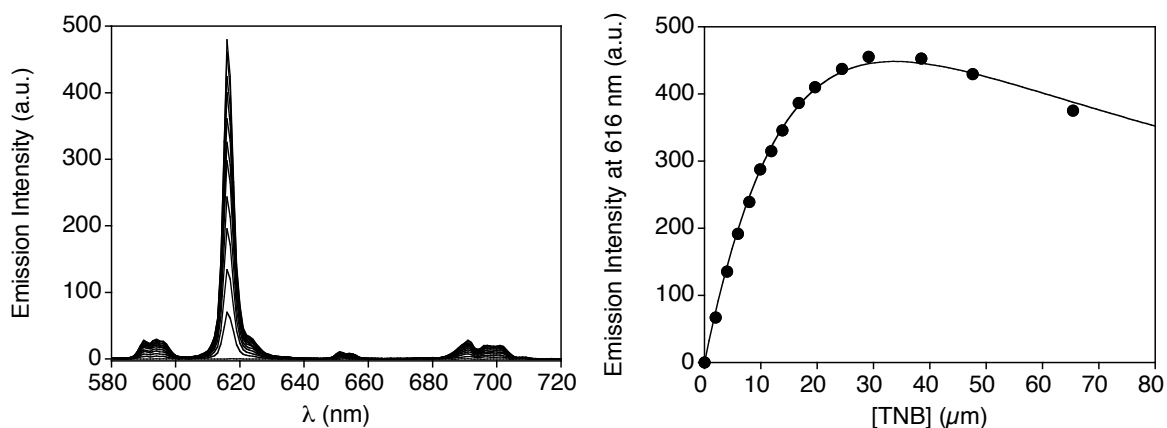


Figure S7. Left: Luminescent spectra of 10 μM $1[\text{Eu}]$ in HEPES buffer (10 mM HEPES, 100 mM NaCl, pH 7.6) adding increasing amounts of **TNB**, $\lambda_{\text{exc}} = 280$ nm. **Right:** Emission at 616 nm of $1[\text{Eu}]$ with increasing amounts of **TNB** and best fit curve to a mixed 1:1 and 1:2 binding model: $K_{D1} \approx 11.3$ μM and $K_{D2} \approx 49.9$ μM .

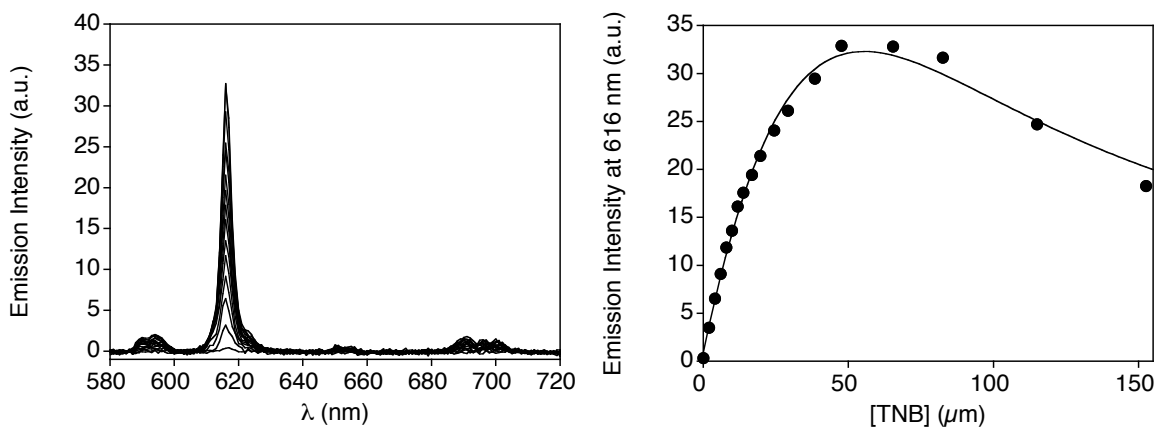


Figure S8. Left: Luminescent spectra of 10 μM $1^{\text{P}}[\text{Eu}]$ in HEPES buffer (10 mM HEPES, 100 mM NaCl, pH 7.6) adding increasing amounts of **TNB**, $\lambda_{\text{exc}} = 280$ nm. **Right:** Emission at 616 nm of $1^{\text{P}}[\text{Eu}]$ with increasing amounts of **TNB** and best fit curve to a mixed 1:1 and 1:2 binding model: $K_{D1} \approx 99.3$ μM and $K_{D2} \approx 22.0$ μM .

Analysis of $1[\text{Eu}] \cdot \text{TNB}$ and $1^{\text{P}}[\text{Eu}] \cdot \text{TNB}$ mixtures by mass spectrometry: In order to rationalize the binding of **TNB** to $1[\text{Eu}]$ and $1^{\text{P}}[\text{Eu}]$, we analyzed by ESI-MS concentrated mixtures of each of the peptides with the **TNB** antenna. For $1[\text{Eu}]$, in addition to the expected $[\text{MH}_2]^{2+}$ and $[\text{MH}_3]^{3+}$ peaks, corresponding to **1** (without the metal), the spectrum showed a clear peak at 933.7 consistent with a complex between a **TNB** antenna and **1**. Likewise, the analysis of the mixture of $1^{\text{P}}[\text{Eu}]$ with **TNB** showed the peak at 974.7 corresponding to a complex between 1^{P} and **TNB**.

These species could arise from an ionic complex between the positively charged peptide and the **TNB** anion, or else from the formation of a condensation product between the diketone and the guanidinium group of an arginine side chain. Similar condensation products have been previously observed in mixtures of peptides and proteins with 1,2-diketones.⁶ In any case, they suggest a secondary binding site for the **TNB** antenna and our sensors.

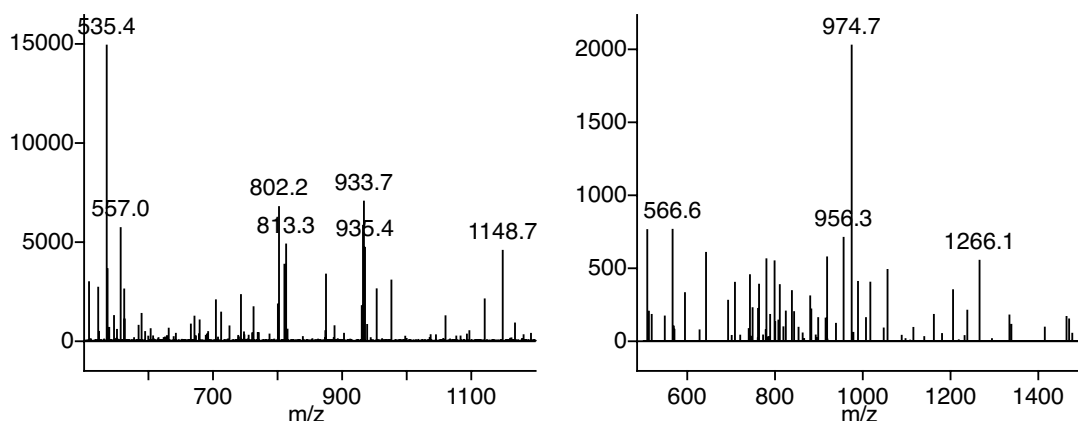


Figure S9. Left: Mass spectrum of an aliquot of a 20 μM solution of $1[\text{Eu}]$ in the presence of 100 μM of **TNB**. 10 mM HEPES, 100 mM NaCl, pH 7.6. The peaks at 802.2 and 535.4 correspond to the $[\text{MH}_2]^{2+}$ and $[\text{MH}_3]^{3+}$ ions of the unphosphorylated peptide **1**. The peak at 933.7 corresponds to the $[\text{MH}_2]^{2+}$ of a $1 \cdot \text{TNB}$ complex. **Right:** Mass spectrum of an aliquot of a 20 μM solution of $1^{\text{P}}[\text{Eu}]$ in the presence of 100 μM of **TNB**. 10 mM HEPES, 100 mM NaCl, pH 7.6. The peak at 974.7 corresponds to the $[\text{MH}_2]^{2+}$ of a $1^{\text{P}} \cdot \text{TNB}$ complex.

⁶ A. Leitner and W. Lindner, *J. Mass Spectrom.*, 2003, **38**, 891.

Influence of the phosphate concentration in the luminescence of the 1[Eu]•TNB complex.

Given the widespread use of phosphate buffers, and the possible interference of their anions in the performance of our sensors, we measured the emission of a 10 μM solution of 1[Eu] in the presence of 40 μM TNB with increasing concentrations of phosphate buffer. The emission intensity was found very robust and even at 9 mM concentration of phosphate was still over 50% of that in absence of phosphate.

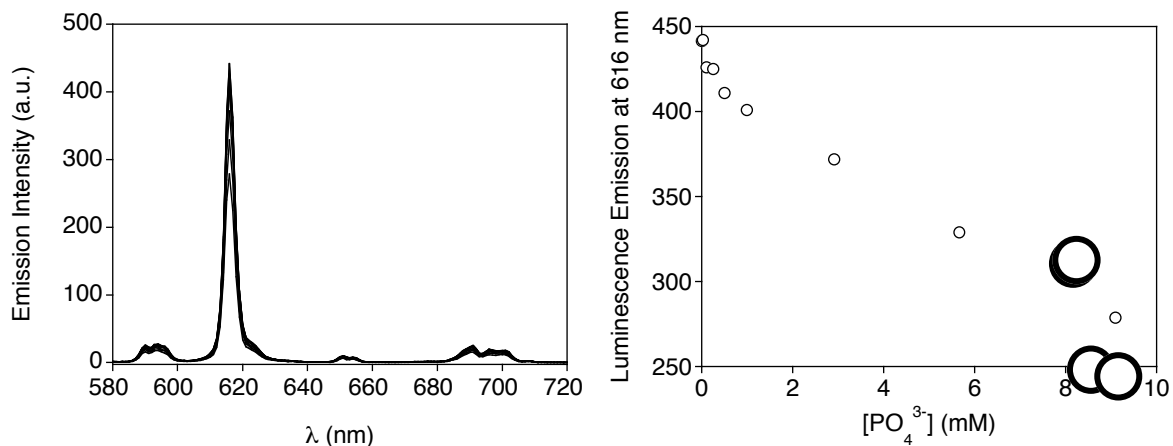


Figure S10. Left: Luminescent spectrum of 10 μM 1[Eu] in HEPES buffer (10 mM HEPES, 100 mM NaCl, pH 7.6) in presence of $\approx 40 \mu\text{M}$ TNB at increasing concentrations of phosphate buffer. Right: Plot of the emission intensity at 616 nm of the same solutions against the total phosphate concentration.

Kinetic experiments with Alkaline Phosphatase (AP): The Calf intestinal AP and the AP 10X buffer were purchased from Promega (Cat. #: M1821).

To 1 mL of a 25 μM solution of $1^{\text{P}}[\text{Eu}]$ in HEPES buffer (10 mM HEPES, 100 mM NaCl, pH 7.6), 8 μL of a 10 mM stock solution of **TNB** in MeOH, 10 μL of Alkaline Phosphatase 10X buffer and 20 μL of Alkaline Phosphatase (1 u/ μL) were added at rt, and the luminescence at 616 nm were recorded every 5 min using *setup 4* parameters.

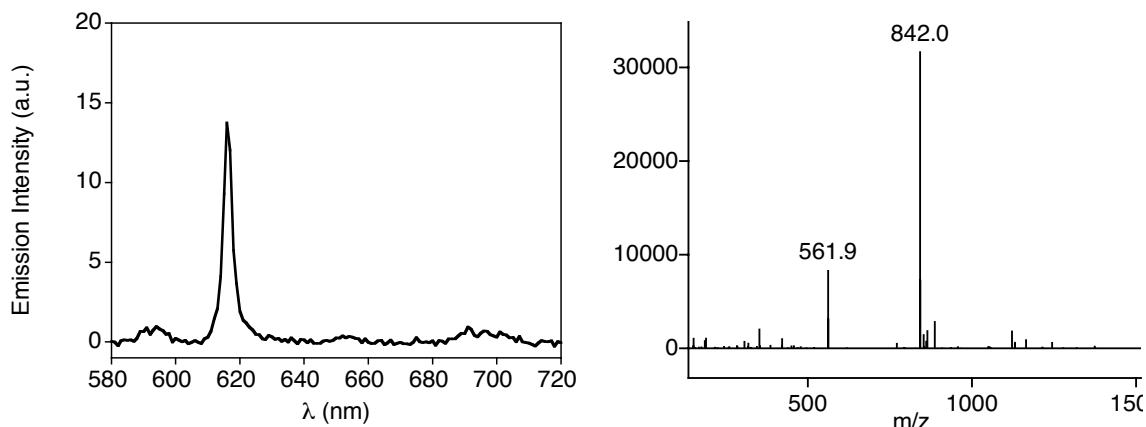


Figure S11. Left: Luminescent spectrum of 25 μM $1^{\text{P}}[\text{Eu}]$ in HEPES buffer (10 mM HEPES, 100 mM NaCl, pH 7.6) in presence of ≈ 78.6 μM **TNB** and 0.1X Alkaline Phosphatase buffer, using *setup 2* parameters with an excitation slit width of 2.5 nm and an emission slit width of 1.5 nm, $\lambda_{\text{exc}} = 280$ nm. Right: Mass spectrum of the sample before addition of AP. Peaks at 842.0 and 561.9 correspond to $[\text{MH}_2]^{2+}$ and $[\text{MH}_3]^{3+}$ ions of 1^{P} .

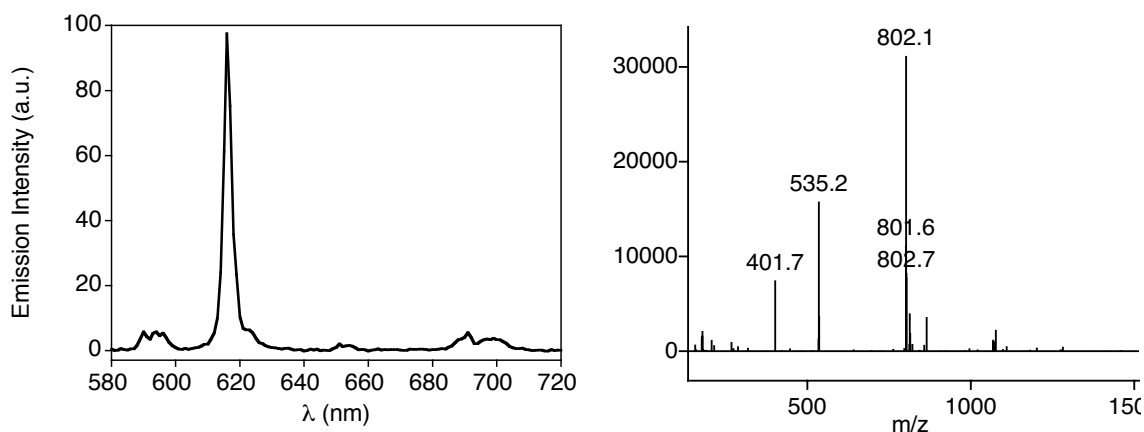


Figure S12. Left: Luminescent spectra of 25 μM $1^{\text{P}}[\text{Eu}]$ in HEPES buffer (10 mM HEPES, 100 mM NaCl, pH 7.6) in presence of ≈ 77 μM **TNB**, 0.1X Alkaline Phosphatase buffer and 20 units of Alkaline Phosphatase after 300 min of reaction, using *setup 2* parameters with an excitation slit width of 2.5 nm and an emission slit width of 1.5 nm, $\lambda_{\text{exc}} = 280$ nm. Right: Mass spectrum of an aliquot of the sample after 300 min of reaction with AP. Peaks at 802.1, 535.2 and 401.7 correspond to $[\text{MH}_2]^{2+}$, $[\text{MH}_3]^{3+}$ and $[\text{MH}_4]^{4+}$ ions of **1**.

Using the parameters determined from simultaneous fitting on the entire set of progress curves for the reaction of different concentrations of $1^P[\text{Eu}]$, we estimate the Michaelis constant $K_m = 14.5 \pm 2.5 \mu\text{M}$ and the product inhibition constant $K_i = 4.4 \pm 0.6 \mu\text{M}$. We determined the binding constant of **TNB** to $1[\text{Eu}]$ from the titration experiment and kept it fixed ($K_{D1} = 11.3 \mu\text{M}$) in the kinetics analysis.

Kinetic experiments with PKC α : The human PKC α was purchased from *ProQinase* (Product. #: 0222-0000-1). ATP, phosphatidylserine and 1,2-dioleoylglycerol were purchased from *Aldrich* (Cat. #: A-7699; P-7769 and D-8394 respectively).

To 1 mL of a 20 μM solution of $1[\text{Eu}]$ in HEPES buffer (20 mM HEPES, 2.5 mM MgCl_2 , 0.225 mM CaCl_2 , 500 μM ATP, 1 mM DTT, 0.5 $\mu\text{g/mL}$ phosphatidylserine, 0.1 $\mu\text{g/mL}$ diacylglycerol, pH 7.4), 8 μL of a 10 mM stock solution of **TNB** in MeOH and 4 μL of PKC α 0.17 $\mu\text{g}/\mu\text{L}$ were added at rt, and the luminescence at 616 nm were recorded every 2 min using *setup 4* parameters changing the excitation wavelength to 290 nm to avoid the interference coming from the absorption of ATP at 280 nm.

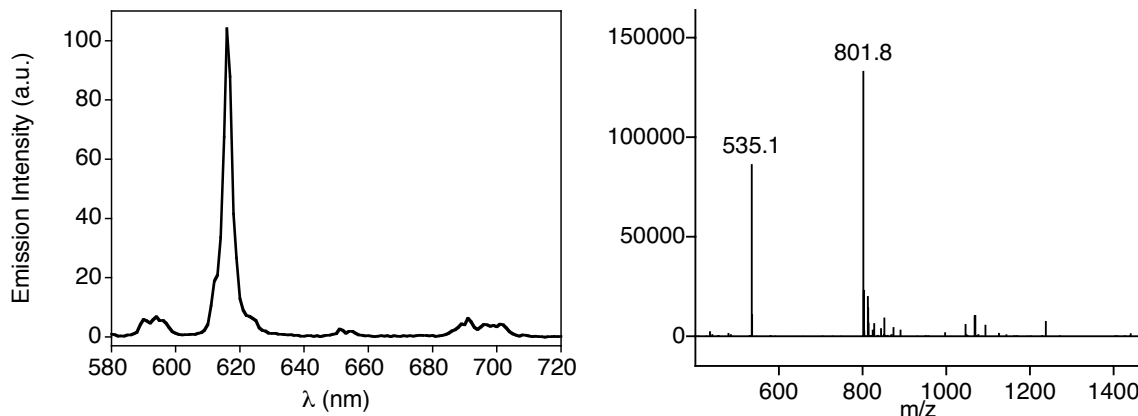


Figure S14. Left: Luminescent spectra of 20 μM $1[\text{Eu}]$ in HEPES buffer (20 mM HEPES, 2.5 mM MgCl_2 , 0.225 mM CaCl_2 , 500 μM ATP, 1 mM DTT, 0.5 $\mu\text{g/mL}$ phosphatidylserine, 0.1 $\mu\text{g/mL}$ diacylglycerol, pH 7.4) in presence of $\approx 79.4 \mu\text{M}$ **TNB**, using *setup 2* parameters with an excitation slit width of 2.5 nm and an emission slit width of 1.5 nm, $\lambda_{\text{exc}} = 290$ nm. **Right:** Mass spectrum of an aliquot of the sample before the addition of PKC α . The peaks at 801.8 and 535.1 correspond to the $[\text{MH}_2]^{2+}$ and $[\text{MH}_3]^{3+}$ ions of the dephosphorylated peptide.

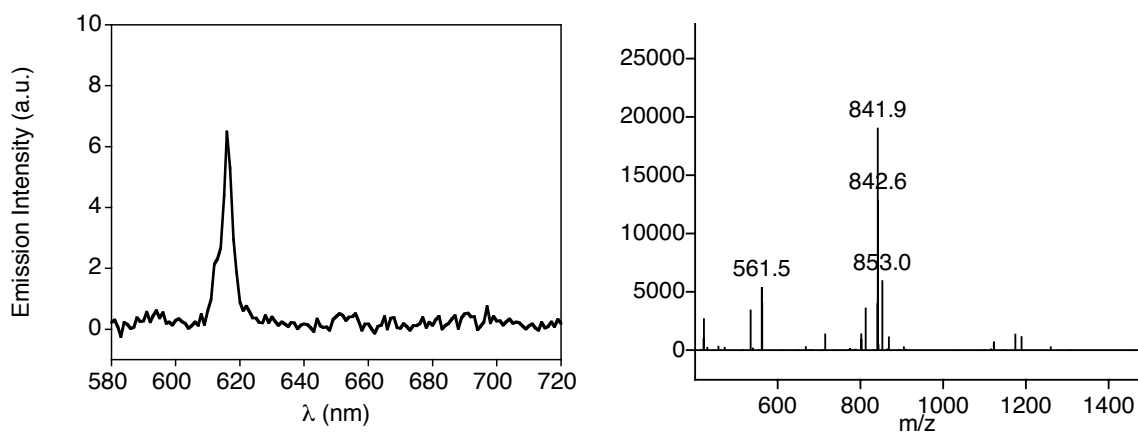
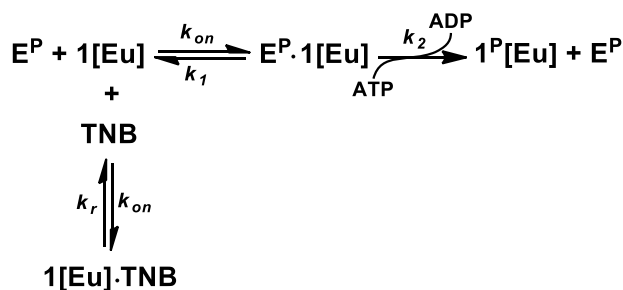


Figure S15. Left: Luminescent spectra of 20 μM **1[Eu]** in HEPES buffer (20 mM HEPES, 2.5 mM MgCl_2 , 0.225 mM CaCl_2 , 500 μM ATP, 1 mM DTT, 0.5 $\mu\text{g/mL}$ phosphatidylserine, 0.1 $\mu\text{g/mL}$ diacylglycerol, pH 7.4) in presence of ≈ 79 μM **TNB** and ≈ 0.7 $\mu\text{g/mL}$ of **PKC α** after 300 min of reaction, using *setup 2* parameters with an excitation slit width of 2.5 nm and an emission slit width of 1.5 nm, $\lambda_{\text{exc}} = 290$ nm. **Right:** Mass spectrum of an aliquot of the sample after 300 min of reaction with **PKC α** . The peaks at 841.9 and 561.5 correspond to the $[\text{MH}_2]^{2+}$ and $[\text{MH}_3]^{3+}$ ions of the phosphorylated peptide.

The same experiment was carried out with 0.5, 1 and 1.5 μM solutions of **1[Eu]**, in the presence of ≈ 10 μM **TNB**, 500 μM ATP, and ≈ 0.17 $\mu\text{g/mL}$ of **PKC α** , using *setup 4* parameters changing the excitation wavelength to 290 nm, the excitation slit width to 5 nm and the emission slit width to 5 nm.

We have analyzed these data using the progress curves of the reaction (shown in Fig. S16). These concentration-time data were fitted for the kinetic parameters defined in the simplest model presentation of this reaction as shown in Scheme S3, using the series of differential equations governing each reaction step. This direct fitting was performed again by using the DynaFit program as previously described. Using the parameters determined from simultaneous fitting on the entire set of progress curves for the reaction of different concentrations of **1[Eu]** and constant 500 μM ATP, we estimate the apparent Michaelis constant for **1[Eu]** $K_m = 0.23 \pm 0.01$ μM . We determined the binding constant of **TNB** to **1[Eu]** from the titration experiment obtained in the same solution mixture as prepared for the kinase assays, and kept it fixed ($K_{DI} = 2.7$ μM) in the kinetics analysis.⁷

⁷ The **1[Eu]**•**TNB** association constant was reevaluated under the kinase assay conditions, and was found slightly better than in HEPES buffer ($K_{DI} = 2.7$ vs. 11.3 μM); likewise, the formation of the **1^P[Eu]**•**TNB** complex was also more favorable under those conditions ($K_{DI} = 31.1$ vs. 99.3 μM). However, in both cases the binding of **TNB** to **1[Eu]** was about ten times more favorable than to **1^P[Eu]**.



Scheme S3. Simplified reaction scheme for the reaction of **1[Eu]** in the presence of human PKC α (E^{P} – ATP bound enzyme) and **TNB** (**1[Eu]**·**TNB** complex emits the luminescence response signal). The regeneration of E^{P} (i.e. dissociation/association of ADP/ATP) is assumed as rapid equilibrium process.

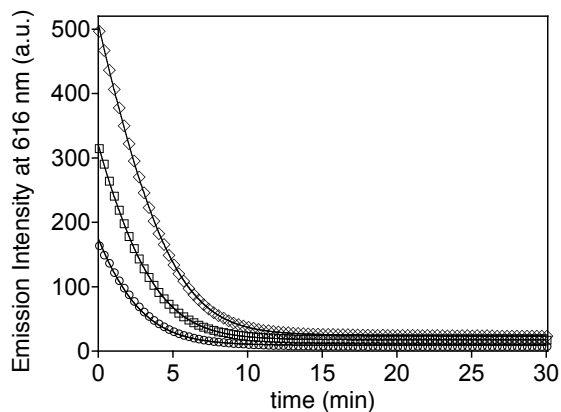


Figure S16. Time courses for 0.5 μM (○), 1 μM (□) and 1.5 μM (◇) solutions of **1[Eu]** in HEPES buffer (20 mM HEPES, 2.5 mM MgCl₂, 0.225 mM CaCl₂, 500 μM ATP, 1 mM DTT, 0.5 μg/mL phosphatidylserine, 0.1 μg/mL diacylglycerol, pH 7.4) in presence of ≈ 10 μM **TNB** and ≈ 0.17 μg/mL of PKC α , $\lambda_{\text{exc}} = 290$ nm.

NMR assays

The NMR spectra were recorded in a *Varian Inova 500* spectrometer.

A 1.84 mM solution of **1^P** in HEPES buffer (10 mM HEPES, 100 mM NaCl, pH 7.6, 0.5 mL) was lyophilized, and the dried residue was redissolved in 0.5 mL of D₂O. This process was repeated 2 times. Finally, the sample was dissolved in 0.5 mL of D₂O.

After recording the spectrum, 4.6 μL of a 0.2 M EuCl₃ solution in D₂O were added to the **1^P** solution (1 equivalent of Eu³⁺). The solution was mixed and after 1 hour the NRM spectrum was recorded.

³¹P NMR of **1^P** and **1^P[Eu]**:

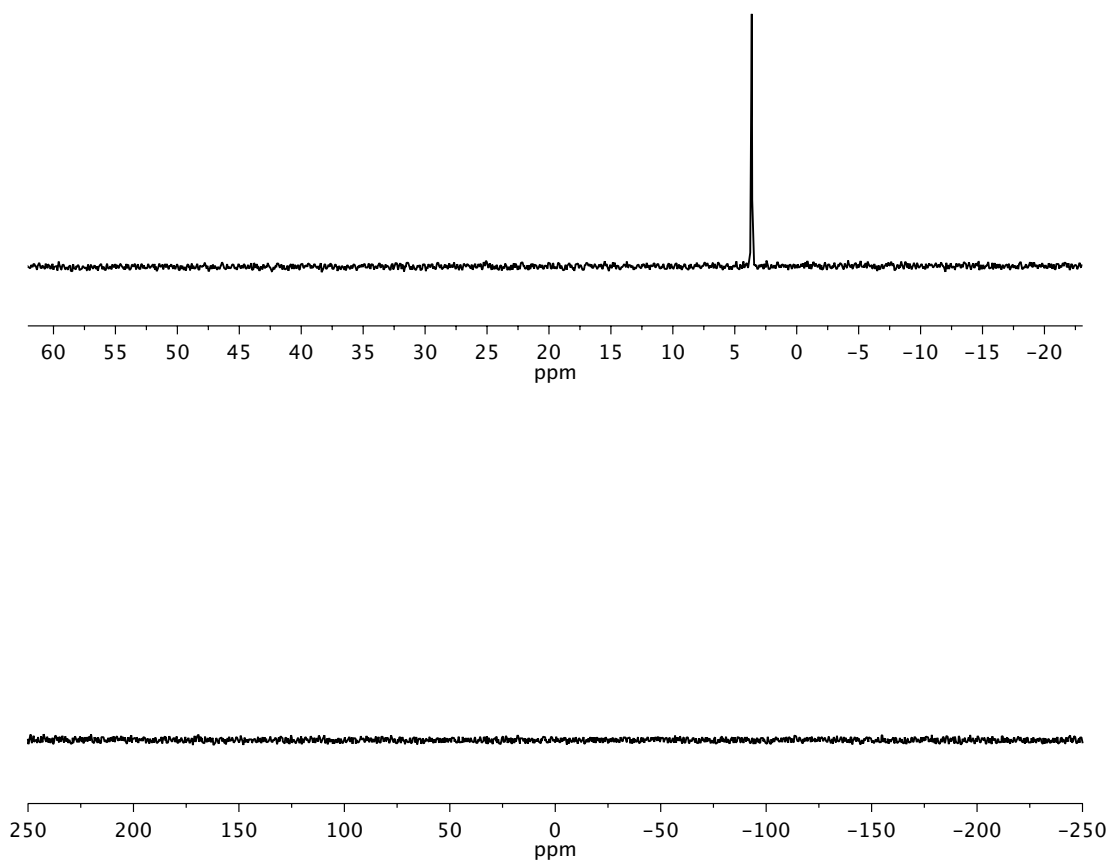


Figure S17. Top: ³¹P NMR spectra of **1^P** in 1.84 mM concentration, in which the peak at 3.63 ppm corresponds with the phosphate group. **Bottom:** ³¹P NMR spectra of **1^P[Eu]** in 1.84 mM concentration, in which the peak at 3.63 ppm has disappeared due to the coordination of the phosphate group with the europium.